EPR studies of electron and hole trapping in titania photocatalysts

I. Ross Macdonald, Shona Rhydderch, Emily Holt, Neil Grant, John M.D. Storey, Russell F. Howe *

Chemistry Department, University of Aberdeen, Aberdeen AB24 3UE, United Kingdom

ABSTRACT

In situ EPR spectroscopy at cryogenic temperatures is used to observe paramagnetic products formed when titania photocatalysts are irradiated with UV–visible light in the presence of reactant molecules. Irradiation in vacuo, in the absence of reactants, produces weak EPR signals of trapped holes (O^-) and trapped electrons (Ti^{3+}). When high photon fluxes are used, the intensities of the trapped electron signals are enhanced dramatically when irradiation is stopped. This process is completely reversible on restoring the irradiation, and is attributed to a trapping of EPR invisible conduction band electrons once irradiation is stopped. The trapped electrons are excited back into the conduction band when irradiation is resumed. In the presence of adsorbed organic compounds, products of valence band hole trapping by the organic molecules are detected. Methyl radicals are formed by attack of valence band holes on adsorbed acetic acid. The valence band holes are also able to cleave carbon–silicon bonds, forming methyl radicals from tetramethylsilane. Benzyltrimethylsilane derivatives form both methyl radicals and benzyl radicals through cleavage of all four carbon–silicon bonds. The relevance of these observations to photocatalysed organic reactions in which carbon–carbon bond formation occurs via radical intermediates is discussed.

© 2011 Elsevier B.V. All rights reserved.

1. Introduction

Photocatalytic reactions are initiated through band-gap photo-excitation of the semiconducting oxide, generating valence band holes and conduction band electrons. It is the subsequent fate of these excitons which determines the outcome of the photocatalytic reaction. They may recombine unproductively. They may be trapped at defect states within the bulk of the semiconductor and hence be unavailable for further reaction. Trapping in surface states may, however, prolong the lifetime of the holes and electrons sufficiently to allow electron transfer to adsorbed reactants, initiating reaction. All of these primary events involve single electrons, which are in principle directly observable by electron paramagnetic resonance (EPR) spectroscopy. EPR spectroscopy is highly sensitive, and can be applied in an in situ manner to observe species during illumination. Although conventional (CW) EPR does not have the time resolution of pulsed laser spectroscopy or time resolved conductivity measurements, it has the real advantage of allowing direct identification of the species being observed, and measurements at temperatures down to 4 K can slow processes which cannot be followed at room temperature.

There is now a substantial literature on the EPR observation of trapped electrons and trapped holes when titania photocatalysts are exposed to band gap radiation. Howe and Graetzel first showed that UV irradiation of aqueous colloidal dispersions of titania in the presence of organic hole scavenging compounds produced EPR signals of electrons trapped at defect Ti^{4+} sites, generating paramagnetic Ti^{3+} [1]. Irradiation of hydrated titania powders in vacuo at low temperature gave EPR signals of trapped electrons plus a signal assigned to valence band holes trapped at lattice oxide ion sites (O^-) [2]. The dynamics of hole and electron trapping in dehydrated nanocrystalline anatase were subsequently investigated in detail by Berger et al. [3–5] who showed that trapping of electrons and holes in this material occurred on a time scale of seconds to minutes at 90 K during in situ irradiation. A discrepancy between the intensities of trapped hole and trapped electron signals was attributed to the presence of delocalised conduction band electrons during irradiation which are EPR silent, but which can be seen as a broad infrared absorption by FTIR spectroscopy.

Electron trapping has also been studied by EPR in the mixed phase titania photocatalyst Degussa P25 [6,7]. Aqueous colloidal suspensions and slurries of P25 on irradiation at low temperature gave EPR signals of trapped electrons (Ti^{3+}) in both the anatase and the rutile components of P25. The key finding in this work was that electron transfer from rutile to anatase slows recombination, generating catalytic hot spots at the anatase:rutile interface.

We have recently described some in situ EPR studies of electron trapping in a nanocrystalline rutile [8]. In this work it was found that narrow band irradiation of rutile with light of energy greater than or equal to the band gap generated, as with anatase, low concentrations of trapped holes and trapped electrons. However, when high intensity broad band irradiation was applied, trapped holes and

* Corresponding author. Tel.: +44 1224 272948; fax: +44 1224 272921.
E-mail address: r.howe@abdn.ac.uk (R.F. Howe).

electrons could scarcely be detected during irradiation at 80 K or 4 K. When the light was turned off, intense trapped electron signals immediately appeared. This process was completely reversible; the trapped electron (Ti^{3+}) signals were removed as soon as broad band irradiation was resumed. The explanation proposed for these observations was that under irradiation there is a dynamic equilibrium established between creation of conduction band electrons, trapping of electrons, and excitation of trapped electrons back into the conduction band. The steady state concentration of trapped electrons depends on the light intensity. When irradiation is stopped, conduction band electrons are trapped and remain so in the dark.

Photocatalytic reactions rely on interception of holes and electrons by adsorbed molecules, which should produce free radicals as initial products. For example, oxygen readily reacts with Ti^{3+} sites (trapped electrons) to form the superoxide ion, O_2^-. Carter et al. have identified four different superoxide species on reduced P25 anatase, attributed to the presence of four different types of adsorption sites on the anatase and rutile surfaces in P25 [9]. Irradiation of titania in the presence of both oxygen and adsorbed ketones produces EPR signals assigned to peroxy type radicals $ROO^\bullet$ [10,11]. The authors of this work suggest that there are three different and competing reaction pathways involved in the oxidative decomposition of ketones over titania under UV irradiation: direct oxidation of the ketone by trapped valence band holes, reduction of the ketone by trapped electrons, and reaction of the ketone with superoxide ions formed from trapped electrons.

In the absence of oxygen, the primary reaction of adsorbed organic molecules is expected to be with valence band holes. Shkrob and Chemerisov have recently described a comprehensive EPR study of light induced reactions of carboxylic, hydrocarboxylic and aminocarboxylic acids, carboxylated aromatics, amino acids and peptides adsorbed on hydrated anatase and iron oxide surfaces in the absence of oxygen [12]. This work found that indeed the dominant reaction pathway was oxidative decarboxylation by valence band holes, generating carbon based radicals. A further key finding was that the reactions occurred directly with trapped holes at the photocatalyst surface, not as a consequence of secondary reactions with hydroxyl radicals formed from hole scavenging by surface hydroxyl groups or adsorbed water. Only in the case of mellitic acid was there evidence for electron scavenging by the adsorbed organic molecule (forming the radical anion of mellitic acid).

In this paper we present some recent results relating to electron trapping in different forms of titania, and our observations of organic radicals relevant to reactions occurring under oxygen free conditions with potential for organic synthesis involving carbon–carbon bond formation.

2. Experimental

Three different titania samples were used in this work. PC500 (Millennium) is a nanocrystalline anatase with a surface area of $300\,m^2\,g^{-1}$. P25 (Degussa) is a composite of anatase (80%) and rutile (20%), with a surface area of $50\,m^2\,g^{-1}$. An experimental nanocrystalline rutile provided by CRODA International PLC is described in Ref. [8]. Samples for EPR experiments were placed in quartz high vacuum cells, or pyrex cells fitted with quartz sidearms. All titania samples were outgassed by evacuation below 10^{-4} mbar overnight. The EPR cells used for the study of organic radicals employed a second side-arm containing a degassed solution of the organic substrate in acetonitrile (typically 1 wt%) which could be added to the titania under vacuum. EPR spectra were recorded on either a JEOL FA200 X-band spectrometer fitted with an Oxford Instruments ESR900 cryostat utilising liquid helium or liquid nitrogen as the refrigerant, or on a Bruker ECS106 X-band spectrometer using a liquid nitrogen insert dewar or variable temperature system

employing liquid nitrogen. In situ irradiation in the JEOL spectrometer used a 450 W LOT Hg(Xe) arc source, focussed onto the sample through a lense built into the JEOL cavity. Pyrex glass (320 nm) and water (900 nm) filters cut off the hard UV and infrared wavelengths, respectively. With the Bruker spectrometer, a 150 W Optosource xenon lamp was focussed onto the irradiation slots on the front of the cavity. Computer simulation of observed spectra employed the Bruker Simfonia program. g-Values were determined by calibration with DPPH (Bruker spectrometer) or manganese (JEOL spectrometer) standards.

Organic reagents acetic acid, tetramethylsilane, and maleic anhydride were Analar grade from Sigma–Aldrich. Analar acetonitrile solvent was dried over CaH_2 in a continuous still. The various benzyltrimethylsilane derivatives were prepared by reaction of chlorotrimethylsilane with the appropriate benzylmagnesium chloride reagent, prepared in situ under nitrogen in dried THF.

3. Results and discussion

3.1. Irradiation of titania in vacuo

The EPR spectra obtained when titania samples are irradiated in vacuo at low temperatures depend on the nature of the titania sample, and on the photon flux incident on the sample. In this work we have found that at low light intensity (e.g. $15\,mW\,cm^{-2}$ from the 150 W xenon lamp) all three titania samples give the signals of trapped holes and trapped electrons reported previously in the literature, which decay very slowly on standing in the dark at 77 K. Very different behaviours are seen when higher light intensities are used. Fig. 1 shows spectra from an experiment in which a nanorutile sample outgassed at room temperature was irradiated with broad band (320–900 nm, $300\,mW\,cm^{-2}$) light in vacuo at 4 K. During irradiation (trace (b)), a very weak Ti^{3+} signal could be seen (not discernable on the scale used in Fig. 1), and any trapped hole signals were obscured by the signal due to defects in the quartz sample tube. The decrease in intensity of this defect signal when the light is turned on is due to a temperature increase under irradiation (from 4 K to ca. 8 K). When the light is turned off, the intense Ti^{3+} signal shown in Fig. 1(c) appears, which is approximately two orders of magnitude more intense than that seen during
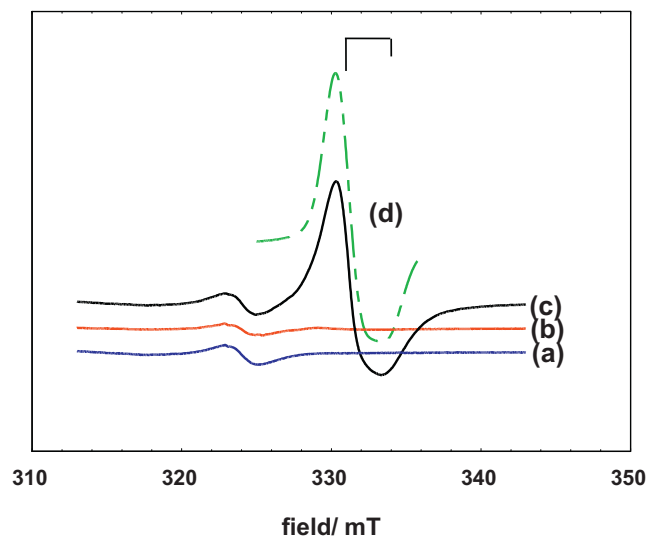

Fig. 1. EPR spectra recorded when nano-rutile is irradiated in vacuo at 4 K with broad band radiation. (a) Initial spectrum in the dark (the signal at 325 mT is due to a defect in the quartz sample tube); (b) during irradiation; (c) 15 min after switching off the light; and (d) computer simulation of the Ti^{3+} signal.

irradiation. The Ti^{3+} signal is dominated by a component which has $g_\perp$ = 1.962 and $g_\parallel$ = 1.944 (verified by the computer simulation in Fig. 1(d)). This signal was tentatively assigned in Ref. [8] to a surface Ti^{3+}OH species, partly because its contribution to the spectrum was greatly diminished when the surface was partially dehydroxylated. As reported in [8], the growth of the trapped electron signal when the light is switched off occurs relatively slowly, with a half-life of ~250 s at 4 K (150 s at 77 K). When the light is switched on again, the Ti^{3+} signal is removed much more rapidly, with a half-life of less than 1 s. Provided no oxygen was present to scavenge the electrons, these processes of electron trapping and de-trapping could be repeated many times in a completely reversible fashion. Results of detailed studies of the kinetics and wavelength dependence of the de-trapping process will be presented elsewhere [13]. The explanation proposed for these effects is that during broad-band irradiation a steady state equilibrium is established between electrons in the conduction band and those in trap sites, involving a balance between excitation from the valence band into the conduction band, trapping as Ti^{3+}, and de-trapping back into the conduction band. At high photon fluxes, most excited electrons are in the conduction band and not seen by EPR until the light is turned off, and they become trapped. At lower photon fluxes, de-trapping is less efficient, and a higher concentration of trapped electrons can be seen by EPR during irradiation.

Fig. 2 shows results of a similar experiment conducted with the PC500 nanocrystalline anatase. In this case, during broad band irradiation (300 mW cm^{-2}) signals of both trapped holes (O$^-$, $g_\perp$ ~ 2.015, $g_\parallel$ ~ 2.004) and trapped electrons (Ti^{3+}, $g_\perp$ = 1.990, $g_\parallel$ = 1.959) are seen (Fig. 2(b)). When the light is switched off, the trapped hole signal is unchanged, but the trapped electron signal increases (Fig. 2(c)). As with rutile, the effect is completely reversible; the spectrum in Fig. 2(b) is restored when the light is switched on again. There are two noticeable differences from rutile however. The Ti^{3+} signal has a different g-tensor from that seen with rutile, and is similar to signals attributed in the literature to interstitial Ti^{3+} in the anatase structure [2,3]. More importantly, the trapped electron signal increases in intensity much less in the dark than that with rutile; only by a factor of 10 under the same conditions.

These differences between anatase and rutile are also evident when the same experiment is conducted with P25 anatase, which is a mixture of 20% rutile and 80% anatase [6,7]. As shown in Fig. 3,

during broad band irradiation trapped hole and trapped electron signals can hardly be seen, but when the light is switched off, signals grow due to trapped electrons. At least three different Ti^{3+} signals are evident in Fig. 3(b), with $g_\perp$ values of 1.990, ~1.98 and 1.962, respectively. The low field component is the Ti^{3+} signal seen in pure anatase. The dominant signal, however, is that obtained with rutile. Comparisons can be made with the detailed studies of P25 photochemistry reported by Hurum et al. [6,7]. These authors irradiated aqueous dispersions of P25 at low temperature, and observed electron trapping in both the anatase and the rutile phases. The rutile Ti^{3+} signal seen by these authors ($g_\perp$ = 1.975) is not identical to the dominant rutile signal seen here, but does agree with the second Ti^{3+} described in [8] which was more evident when rutile was irradiated at lower light intensities. This second rutile signal also appears to be present (as a poorly resolved shoulder) in Fig. 3.

Further studies of the kinetics and wavelength dependence of these electron trapping processes in P25 are in progress. It is clear, however, that high power irradiation of both anatase and rutile in vacuo, in the absence of any added hole scavengers, produces high concentrations of trapped electrons when the light is switched off. Rutile appears to contain more electron trapping sites than anatase, so that the rutile trap sites dominate the spectra of mixed phase P25, even although anatase is the major phase in this form of titania.

A crucial question for photocatalysis is: what has happened to the valence band holes in these experiments? In principle, one valence band hole is formed for every trapped electron detected by EPR, but the corresponding trapped hole (O$^-$) signals are barely detected in rutile samples, and have much lower intensity than the trapped electron signals in anatase. A final answer to this question is not yet available, but several possibilities may be considered. We view formation of an EPR invisible O$^-$ species as unlikely. The unpaired electron in O$^-$ occupies a 2p orbital which is split from the other two fully occupied 2p orbitals by the surrounding crystal field [14]. Only in the event of this crystal field splitting becoming extremely small might the EPR signal become broadened beyond detection by very rapid spin lattice relaxation. Likewise, trapping of two holes on adjacent oxide ions seems unlikely. The most plausible explanation for the absence of trapped holes in our view is that on these fully hydroxylated titania surfaces valence band holes react with surface hydroxyl groups to form hydroxyl radicals which immediately dimerise, forming hydrogen peroxide. We note that partial dehydroxylation of the rutile samples by heating in vacuo
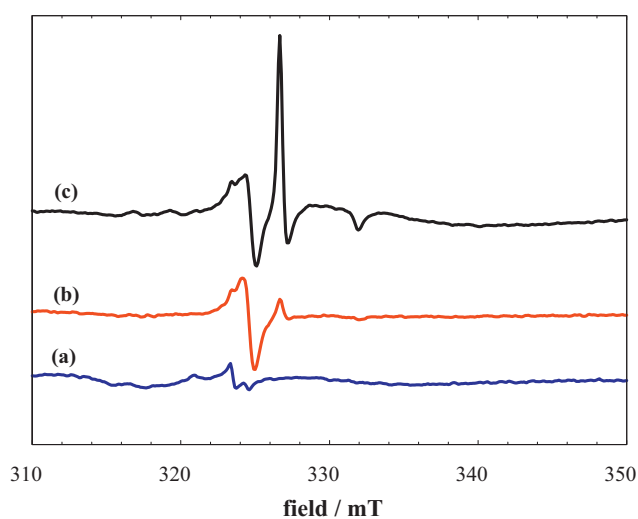

Fig. 2. EPR spectra recorded when anatase (PC500) is irradiated in vacuo at 80 K with broad band radiation. (a) Initial spectrum; (b), during irradiation; and (c) 15 min after switching off the light.
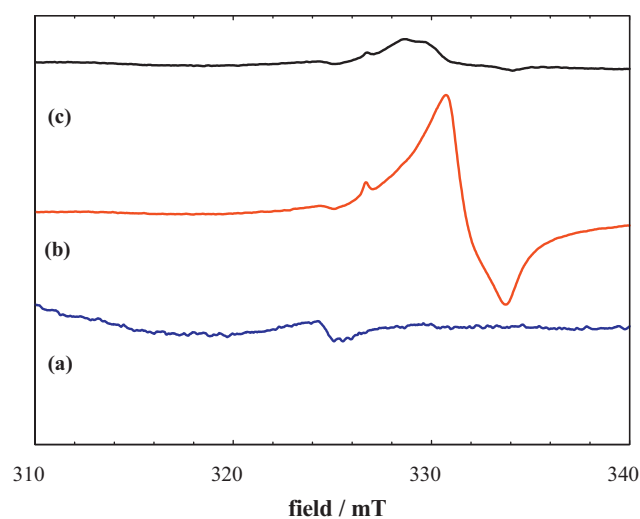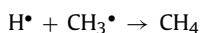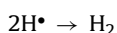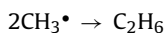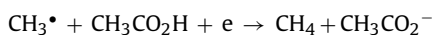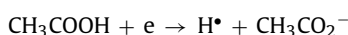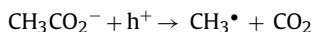

Fig. 3. EPR spectra recorded during (a) and after (b) irradiation of anatase (P25) in vacuo at 80 K with broad band radiation. (c) Spectrum recorded at 80 K after brief warming of (b) to room temperature.

dramatically reduces the intensities of the Ti^{3+} EPR signals obtained following irradiation, which could be due to a reduction in the number of hole trapping sites. Nakamura and Nakato have reported in situ FTIR evidence for formation of TiOOTi and TiOOH species on the surface of UV irradiated rutile suspensions in water, and they propose a mechanism for oxygen photoevolution from such systems initiated by nucleophilic attack of a water molecule on a hole trapped at a surface oxide ion rather than direct oxidation of surface hydroxyl groups by valence band holes. [15] Hydroxyl radicals on the surface of titania have never been directly detected by EPR, even at 4 K, although their presence in aqueous dispersions has been inferred from spin trapping experiments [16]. Further study of these possibilities is on-going. In the second part of this paper, however, we show how valence band holes can be trapped by adsorbed organic molecules, where the evidence comes from direct EPR observation of the organic radical products.

A referee has drawn to our attention to a time-resolved optical spectroscopic study of photoinduced electron detrapping in aqueous dispersions of titania nanoparticles [17]. In that work, 532 nm or 1064 nm photoexcitation of trapped electrons generated by 355 nm photolysis of the titania caused rapid photobleaching of their absorption band in the visible and near IR. This was attributed to promotion of trapped electrons into the conduction band followed by rapid recombination with trapped holes. The EPR experiments in the present work detect very few trapped holes, so that recombination of the promoted electrons is not a major pathway, and the detrapping–trapping process is reversible.

3.2. Photo-reaction of acetic acid

The photo-Kolbe reaction of acetic acid over titania powders is well known, producing a mixture of methane, ethane, carbon dioxide and hydrogen. Kraeutler and Bard [18] proposed the following mechanism for the reaction, involving trapped holes and trapped electrons produced on UV irradiation of the titania:

$$CH_3CO_2^- + h^+ \rightarrow CH_3^\bullet + CO_2$$

$$CH_3COOH + e \rightarrow H^\bullet + CH_3CO_2^-$$

$$CH_3^\bullet + CH_3CO_2H + e \rightarrow CH_4 + CH_3CO_2^-$$

$$2CH_3^\bullet \rightarrow C_2H_6$$

$$2H^\bullet \rightarrow H_2$$

$$H^\bullet + CH_3^\bullet \rightarrow CH_4$$

Evidence for the intermediacy of methyl radicals in this reaction was first obtained from spin trapping EPR experiments. More recently, direct EPR observation of methyl radicals was achieved in aqueous dispersions of platinised titania. These studies also detected the carboxymethyl radical, $^\bullet CH_2COOH$ [19,20].

Fig. 4 shows EPR spectra measured in this work when P25 titania contacted with a degassed solution of acetic acid in acetonitrile was irradiated in situ at 80 K. The spectrum obtained during initial irradiation is dominated by a 1:3:3:1 quartet with a splitting of 2.3 mT assigned to methyl radicals. These are presumed to be formed by attack of valence band holes on adsorbed acetic acid, following previous literature. It should be noted that trapped electron signals (Ti^{3+}) can scarcely be seen, even when the light is switched off (Fig. 4(b)). This is an important point; it means that electrons are also participating in the reaction pathway and not remaining trapped.

When acetic acid-d_4 is used in the same experiment, the methyl radical quartet is replaced by a 7-line pattern (splitting $\sim$ 0.3 mT)
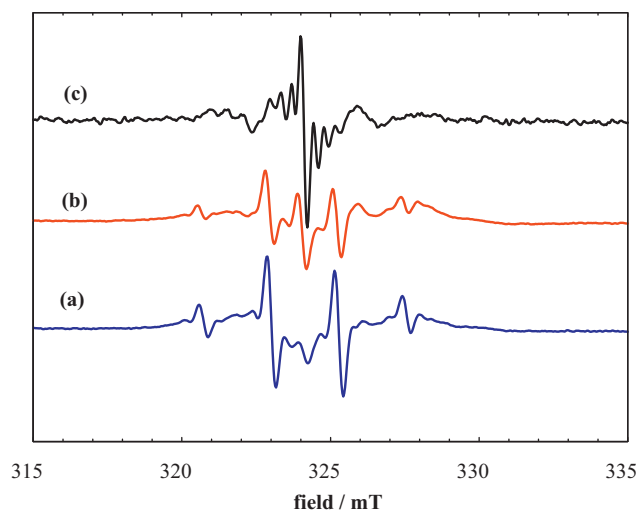

Fig. 4. EPR spectra recorded when P25 anatase is irradiated in the presence of adsorbed acetic acid at 80 K. (a) During irradiation of adsorbed acetic acid; (b) after irradiation for 30 min; and (c) during irradiation of acetic acid-d_4.

due to the CD_3 radical, shown in Fig. 4(c). Closer inspection of the spectra reveals that a second signal underlies the CH_3 and CD_3 signals which is more evident after prolonged irradiation. The origin of this signal is not yet fully clear, although we note that the same signal is obtained with both acetic acid and acetic acid-d_4, suggesting that it is not the carboxymethyl radical observed in the aqueous dispersion studies of Refs. [19,20]. The second signal does resemble that attributed by Shkrob and Chemerisov to the cyanomethyl radical $^\bullet CH_2CN$ [12], formed in their case by hole-mediated decarboxylation of cyanoacetic acid, but further studies are in progress with isotopically labelled acetonitrile solvent to confirm that suggestion.

Considering the mechanism of the photo-Kolbe reaction proposed by Kreutler and Bard, these in situ experiments at 80 K confirm that valence band hole attack on adsorbed acetic acid generates methyl radicals. The absence of a significant trapped electron signal following irradiation in the presence of adsorbed acetic acid may also support the proposed second step above involving electron attack on a second adsorbed acetic acid molecule. No hydrogen atoms were observed by EPR, but recombination of these may be rapid at 80 K, and experiments at lower temperatures are needed to confirm this step.

3.3. Photo-reactions of silanes

The use of carboxylic acids as precursors to alkyl or other carbon based radicals through the titania mediated decarboxylation by valence band holes now seems well established. The use of photocatalysis more generally to promote carbon–carbon bond forming reactions which are useful in organic synthesis is also attracting interest. Conventional radical generating reagents in organic synthesis such as tributyltin hydride suffer drawbacks such as toxicity and difficulty of handling [21]. Titania photocatalysts, however, are capable of generating free radicals under much more benign conditions. The group of Hoffmann has reported addition of tertiary amines to electron deficient alkenes photocatalysed by titania [22]. Here we describe an EPR investigation of a synthetic reaction reported by Cermenati et al. [23], in which benzyltrimethylsilane derivatives react with electron deficient alkenes promoted by a titania photocatalyst. Fig. 5 shows the reaction scheme proposed by Cermenati et al. to account for the observed product. Valence band holes attack the benzyltrimethylsilane molecule forming a silicon centred cation which then cleaves the silicon–benzyl bond to form
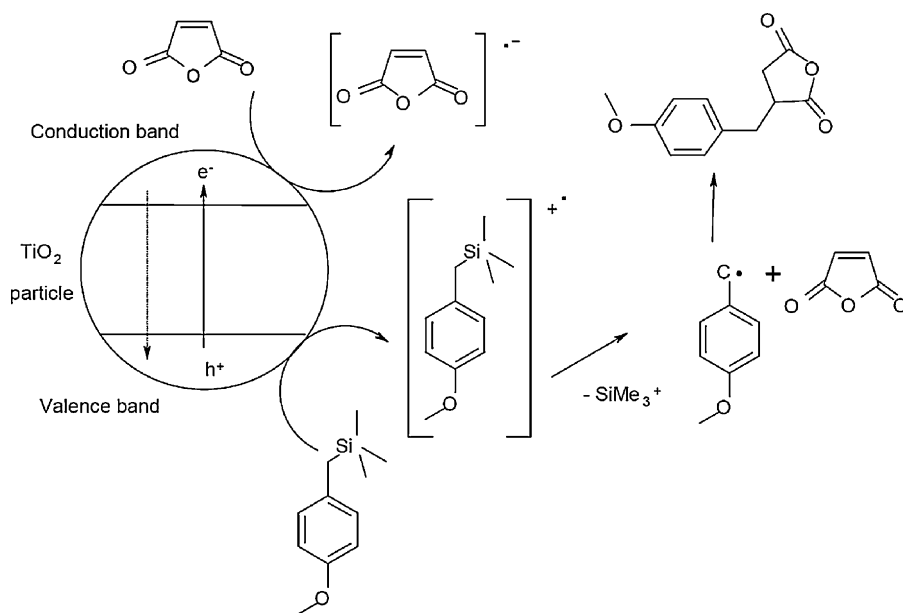
Fig. 5. Scheme showing proposed mechanism of photocatalysed reaction of 4-methoxybenzyltrimethylsilane with maleic anhydride, from Ref. [23].

the benzyl radical (note that in the published scheme the benzyl radical is represented as Ar–C• when what is meant is Ar–CH$_2$•). The maleic anhydride reagent, being electron deficient, was considered to act as an electron scavenger to form the corresponding radical anion. A proposed subsequent attack of the benzyl radical on either the maleic anhydride radical anion or a neutral maleic anhydride molecule then forms the observed reaction product.

We have reported elsewhere our investigations of reaction yields and kinetics for this reaction when conducted in a stirred slurry microreactor [24].

4-Methoxybenzyltrimethylsilane was found to be the most reactive benzyl compound, and the reaction proceeded to completion with 100% selectivity after 6–10 h of reaction at room temperature. The reaction did proceed to a lesser extent with the unsubstituted benzyltrimethylsilane. Rigorous exclusion of oxygen was essential to avoid formation of oxidised by-products. Here we present EPR studies of this system, which provide evidence for some (but not all) of the reaction steps proposed in Ref. [23] (Fig. 5).

Fig. 6 shows EPR spectra recorded when P25 anatase is irradiated (15 mW cm^{-2}) at 77 K in the presence of 4-methoxybenzyltrimethylsilane, maleic anhydride and acetonitrile solvent. The spectrum appearing on initial irradiation (Fig. 6(b)) shows the characteristic 1:3:3:1 quartet of methyl radicals, plus the Ti^{3+} signals due to electrons trapped in the anatase and rutile phases of the P25, respectively. On further irradiation, the methyl radical signal is unchanged, but the trapped electron signals grow in intensity, and a second organic radical signal appears under that of the methyl radicals. On warming to room temperature, all signals were lost.

The origin of the methyl radicals was shown to be the trimethylsilyl group by observing the same signals when the unsubstituted benzyltrimethylsilane was used, and by the observation of no EPR signals at all in a blank experiment with acetonitrile. Irradiation of 4-methoxybenzyltrimethylsilane and acetonitrile with titania in the absence of maleic anhydride gave similar spectra to those shown above. Fig. 7 shows spectra obtained when P25 anatase was irradiated at 77 K in the presence of maleic anhydride and acetonitrile. In this case no organic radicals are detected, but both types of trapped electron (anatase and rutile) are seen, plus a broad and poorly resolved trapped hole signal. It is noteworthy here that maleic anhydride does not scavenge trapped electrons

to produce a radical anion, as suggested in Ref. [23]. On the contrary, the trapped electron signals are enhanced in the presence of maleic anhydride, suggesting that maleic anhydride is acting as a hole scavenger (although no radical products are detected by EPR).

An experiment in which the titania was irradiated in the presence of tetramethylsilane confirmed that the valence band holes in titania are able to cleave Si–CH$_3$ bonds. Spectra obtained in this experiment contained the same methyl radical quartet seen with the benzyltrimethylsilane derivatives.

To investigate further the second organic radical signal appearing when 4-methoxybenzyltrimethylsilane and maleic anhydride are irradiated together at 77 K, the same experiment was undertaken at higher temperature. Fig. 8 shows spectra obtained.

On initial irradiation at 130 K the methyl radical quartet can still be seen, but with much lower intensity than at 77 K. With increasing irradiation time, the methyl radical signal disappears, and the
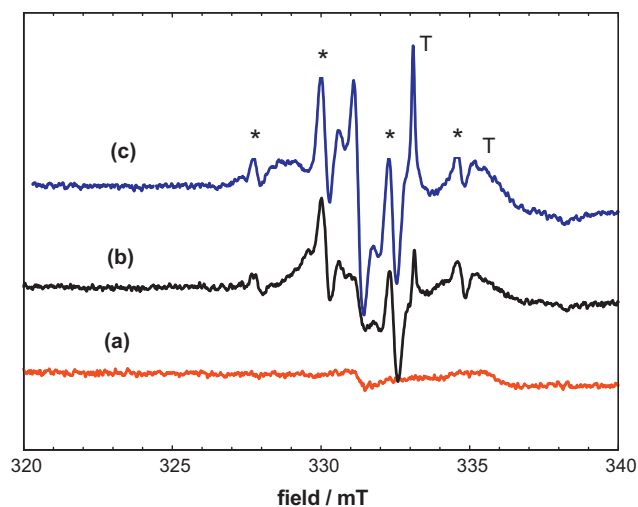

Fig. 6. EPR spectra recorded when anatase (PC500) is irradiated in the presence of adsorbed 4-methoxybenzyltrimethylsilane and maleic anhydride at 77 K. (a) Prior to beginning irradiation; (b) immediately after switching on UV irradiation; and (c) after irradiation for 100 min. *Signal of methyl radicals, and T the signals of trapped electrons (Ti^{3+}).
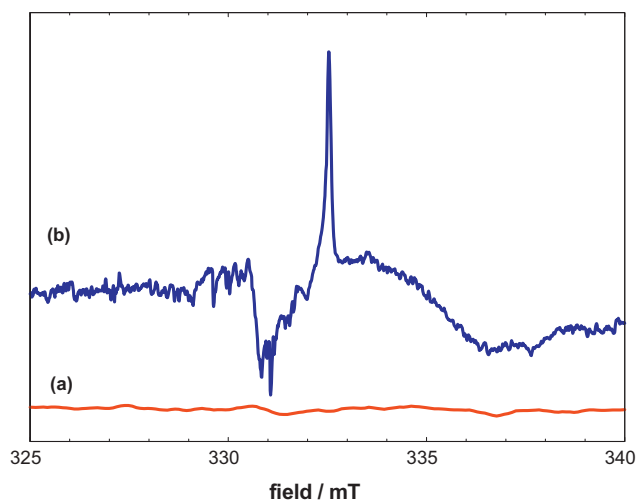
Fig. 7. EPR spectra recorded before (a) and after (b) irradiation of anatase (P25) in the presence of adsorbed maleic anhydride.

Fig. 9. Comparison of observed and simulated spectra of the *o*-methoxybenzyl radical.

trapped electron signals are reduced in intensity, leaving the second organic radical signal more clearly resolved. We assign this second signal to the 4-methoxybenzyl radical. Hyperfine coupling data for a range of different benzyl radicals has been reported by Dust and Arnold [25]. For the 4-methoxybenzyl radical they quote proton couplings of 1.58 mT for the CH_2 protons, 0.5 mT for the two ortho aromatic protons and 0.16 mT for the two meta aromatic protons. Fig. 9 compares the observed spectrum with a best fit simulated spectrum using proton couplings of 1.62 mT (CH_2) and 0.47 (*o*-CH). The satisfactory agreement between these (except where overlapped by the residual trapped electron (Ti^{3+}) signals) confirms the assignment.

In principle, electron transfer (hole attack) could also occur at the methoxy group of *o*-methoxybenzyltrimethylsilane, forming an R-OCH$_2$• radical. Similar EPR spectra to those shown in Figs. 8 and 9 were obtained, however, when the unsubstituted benzyltrimethylsilane was used, suggesting strongly that hole attack occurs at the carbon–silicon bond preferentially.

These EPR studies have revealed several points relevant to the mechanism of the reaction proposed by Cermenati and Albini (Fig. 6). Our obser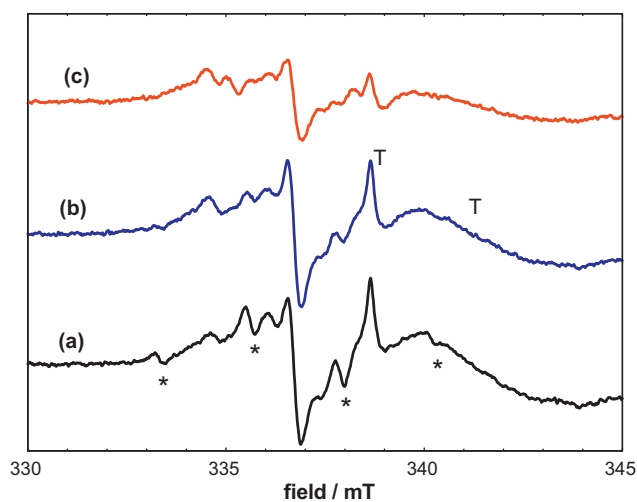vation of the benzyl radical confirms the proposed formation of this species by attack of valence band holes on the benzyltrimethylsilane precursors. The fact that this happens in frozen solution at 77 K or 130 K means that the radical is formed at the titania surface rather than in the solution phase. All 4 carbon–silicon bonds around the silane centre are broken by the reaction with valence band holes, although the methyl radical signal appears more quickly than that of the benzyl radical at 77 K, and the methyl radical is less stable than the benzyl radical at 130 K. However, there is no evidence from the EPR experiments for formation of the maleic anhydride radical anion [26].

Shkrob and Chemerisov have suggested that the mode of adsorption of an organic reactant to the titania surface determines whether or not effective hole transfer and radical formation occurs [12]. If the organic molecule is not strongly enough adsorbed on the titania surface, electron transfer cannot occur. If interfacial charge transfer does occur but produces a particularly stable trapped hole adduct which does not fragment, no organic radical will be seen. In this case, the excess positive charge stays on the surface and can be neutralised by recombination, so that the only persistent paramagnetic species which are detected by EPR are the electrons and holes trapped by the titania [12]. These conclusions were drawn from a range of different types of carboxylic acids, but we suggest that a similar explanation may apply to maleic anhydride.

4. Conclusions

This work has shown that the electron trapping behaviour previously reported for nano-rutile irradiated in vacuo [8] is also seen with pure anatase and with the mixed phase photocatalyst P25. The dynamics of electron trapping and de-trapping under continuous irradiation depend on the photon flux and on the number of trap states available, which can be expected to vary with particle morphology, crystalline phase and crystallinity, and the possible presence of impurities. We have shown here that in situ EPR spectroscopy can follow these processes, and further work is in progress.

We have further confirmed by in situ measurements the conclusions drawn from the ex situ studies of Shkrob and Chemerisov that adsorbed acetic acid traps valence band holes and forms methyl radicals, although the in situ measurements suggest that further reaction of methyl radicals with the solvent may also be occurring.

Finally, the in situ studies have confirmed the proposed benzyl radical formation in the photocatalysed reaction of benzyltrimethylsilanes with maleic anhydride. No evidence has been obtained for electron trapping by maleic anhydride, but the EPR

Fig. 8. EPR spectra recorded during UV irradiation of anatase (P25) in the presence of *o*-methoxybenzyltrimethylsilane and maleic anhydride at 130 K for (a) 1 min; (b) 5 min; and (c) 60 min. *Methyl radical signal, and T the signals of trapped electrons.
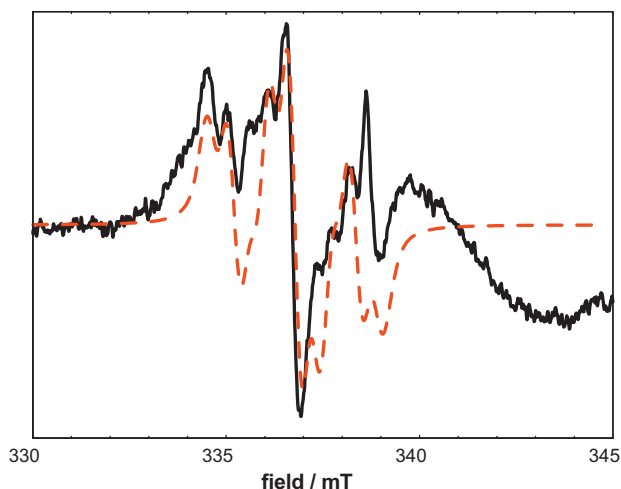
measurements strongly indicate that benzyl radical formation occurs by direct electron transfer at the photocatalyst surface.

Acknowledgements

References

[1] R.F. Howe, M. Graetzel, J. Phys. Chem. 89 (1985) 4495.
[2] R.F. Howe, M. Graetzel, J. Phys. Chem. 91 (1987) 3906.
[3] T. Berger, M. Sterrer, O. Diwald, E. Knoezinger, D. Panayatov, T.L. Thompson, J.T. Yates, J. Phys. Chem. B 109 (2005) 6061.
[4] T. Berger, M. Sterrer, O. Diwald, E. Knoezinger, ChemPhysChem 6 (2005) 2104.
[5] T. Berger, O. Diwald, E. Knoezinger, M. Sterrer, J.T. Yates, Phys. Chem. Phys. 8 (2006) 1822.
[6] D.C. Hurum, A.G. Agrios, K.A. Gray, T. Rajh, M.C. Thurnauer, J. Phys. Chem. B 107 (2003) 4545.
[7] D.C. Hurum, A.G. Agrios, S.E. Crist, K.A. Gray, T. Rajh, M.C. Thurnauer, J. Electron Spectrosc. 150 (2006) 155.
[8] I.R. Macdonald, R.F. Howe, X. Zhang, W. Zhou, J. Photochem. Photobiol. A 216 (2010) 238.
[9] E. Carter, A.F. Carley, D.M. Murphy, J. Phys. Chem. C 111 (2007) 10630.
[10] A.L. Attwood, J.L. Edwards, C.C. Rowlands, D.M. Murphy, J. Phys. Chem. A 107 (2003) 1779.
[11] E. Carter, A.F. Carley, D.M. Murphy, ChemPhysChem 8 (2007) 113.
[12] I.A. Shkrob, S.D. Chemerisov, J. Phys. Chem. C 113 (2009) 17138.
[13] I.R. Macdonald, R.F. Howe, to be published.
[14] M. Che, A.J. Tench, Adv. Catal. 31 (1982) 77.
[15] R. Nakamura, Y. Nakato, J. Am. Chem. Soc. 126 (2004) 1290.
[16] C.D. Jaeger, A.J. Bard, J. Phys. Chem. 83 (1979) 3146.
[17] I.A. Shkrob, M.C. Sauer, J. Phys. Chem. B 108 (2004) 12497.
[18] B. Kraeutler, A.J. Bard, J. Am. Chem. Soc. 100 (1978) 5985.
[19] M. Kaise, H. Nagai, K. Tokuhashi, S. Kondo, Langmuir 10 (1994) 1345.
[20] Y. Nosaka, M. Kishimoto, J. Nishino, J. Phys. Chem. B 102 (1998) 10279.
[21] M.J. Perkins, Radical Chemistry: The Fundamentals, Oxford University Press, New York, 2000.
[22] S. Marinkovic, N. Hoffmann, Eur. J. Org. Chem. (2004) 3102.
[23] L. Cermenati, C. Richter, A. Albini, Chem. Commun. (1998) 805.
[24] N. Grant, J.M.D. Storey, R.F. Howe, Stud. Surf. Sci. Catal. 172 (2007) 445.
[25] J.M. Dust, D.R. Arnold, J. Am. Chem. Soc. 105 (1983) 1221.
[26] K.S. Chen, T. Foster, J.K.S. Wan, J. Phys. Chem. 84 (1980) 2473.